



PARABOLIC MOTION EFFECTS ON CONVECTIVE HEAT AND MASS TRANSFER FLOW OVER A VERTICAL PLATE WITH CROSS DIFFUSION

K. JANARDHAN and S. VENKATA RAMI REDDY

Department of Mathematics
Annamacharya Institute of Technology
and Sciences, Rajampet
Kadapa (Dist.), Andhra Pradesh, India

Department of Mathematics
Sanskriti School of Engineering
Puttaparthi (Dist.), Andhra Pradesh, India

Abstract

The present studied of the problem is scientific investigation of parabolic motion effects on heat and mass flow temperature changes done with a perpendicular to the horizontal plate with cross diffusion and taking an account of the so ret and du four effects. Against the gravitational field the plate is started parabolic with a velocity in its own plane, the plate temperature and concentration is raised up homogeneously with time. The dimensionless prevailing calculations are explained by explicit finite difference technique. Now discussion about the characteristics of the fluid flows through graphically.

Introduction

In situation, there happen flows which are created the temperature variances in addition to the concentration variances. The pace of heat transfer disaffected the rate of mass transfer variances. In trades, several air

2020 Mathematics Subject Classification: 06D99, 06D72, 06D15, 08A72.

Keywords: Pseudo-Complemented Almost Distributive Fuzzy Lattice (PCADFL); Congruence; Minimal prime ideal; Filter; Congruence kernel.

Received October 28, 2021; Accepted November 15, 2021

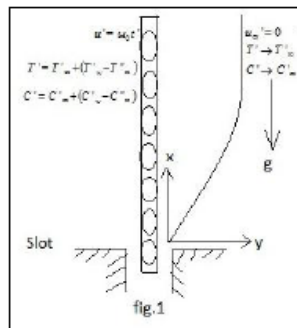
techniques occur in which heat and mass transfer earnings place simultaneously as a result of mutual buoyancy moment in the presence of thermal radiation. In advanced manufacturing for the project of fins, brace rolling, atomic control plants, air turbines and several force gadgets for flying machine, military hardware, digital television, flaming and boiler firm, supplies handling, energy use, temperature quantities, health and military applications heat and mass transfer acts as a vital role.

Many submissions for the parabolic motion like solar cookers, solar concentrators and parabolic trough solar collector. A parabolic concentrator kind solar cooker has a wide range of applications like baking, roasting and distillation due to its exclusive property of creating a practically complex temperature. Muthucumaraswamy et al. [8] are discussed an analytical study of free convection flow near a parabolic in progress endless straight up plate with isothermal in the existence of uniform mass flux. Muthucumaraswamy et al. [3] are scrutinized the MHD convection free flow with a starting explanatory movement of an countless isothermal perpendicular to the horizontal plate in the presence of thermal radiation and chemical reaction. Muthucumaraswamy et al. [2] are studied the flow of preceding a starting parabolic motion of the countless perpendicular to the horizontal plate with adjustable temperature and flexible mass diffusion. Prabhakar Reddy et al. [9] examined numerical the effects of chemical radiation reaction on an unstable HMD free flow convection with a starting parabolic motion of an unlimited isothermal perpendicular to the horizontal porous plate and considering the effect of viscous dissipation. Muthucumaraswamy et al. [6] extended the pivot impacts on an uneven incompressible stream of an electrically leading past liquid homogeneously enhanced vast isothermal perpendicular to the horizontal plate, under the activity of a transitionally applied attractive field. Muthucumaraswamy et al. [7] illuminated trembling past a flow starting parabolic motion of the boundless perpendicular isothermal to the horizontal plate uniform mass dispersion, within the sight of a chemical homogeneous response of the major edict. Soundalgekar [11] is explained the viscous incompressible flow past fluid vast perpendicular to the horizontal uniformly accelerated plate in the straight up direction. Singh et.al [10] elucidated the impact of free-convection mass exchange viscous incompressible flow past fluid an accelerated uniformly countless

perpendicular to the horizontal plate. Hossain et al. [1] are investigated the free-convection laminar unsteady flow of a incompressible fluid viscous, an accelerated endless porous plate perpendicular to the horizontal. Muthucumaraswamy et al. [4] examined the variable temperature and mass diffusion unsteady hydro magnetic past flow of uniformly accelerated infinite perpendicular to the horizontal porous plate. Muthucumaraswamy et al. [5] surveyed the impacts of turn on the unsteady flow past fluid of a uniformly incompressible accelerated endless perpendicular to the horizontal plate with flexible Temperature and Diffusion of Mass.

Design of the problem:

Two-dimensional non-consistent flow of a viscous incompressible fluid past an endless vertical plate with parabolic started motion in the presence of dufour and soret effects has been considered. The axis of x plate is taken perpendicular to the horizontal axis, and the axis of y plate is taken parallel to the horizontal axis. At time, $t' \leq 0$, temperature T'_∞ and concentration C'_∞ are same at the plate and fluid, $t' > 0$, the plate velocity is started Parabolic $u = u_0 t'^2$ in a plane of its own contrary to field of gravitational. Near the plate the temperature and concentration linearly raised up with time. Now the Boussinesq's approximations in non-dimensional form of the unstable flow fluid are represented by the accompanying conditions:



Momentum conservation

$$\frac{\partial U}{\partial t} = \frac{\partial^2 U}{\partial Y^2} + G_r \theta + G_c C \tag{1}$$

Energy conservation

$$\frac{\partial \theta}{\partial t} = \frac{1}{P_r} \frac{\partial^2 \theta}{\partial Y^2} + D_f \frac{\partial^2 C}{\partial Y^2} \quad (2)$$

Species conservation

$$\frac{\partial C}{\partial t} = \frac{1}{S_c} \frac{\partial^2 C}{\partial Y^2} + S_r \frac{\partial^2 \theta}{\partial Y^2} \quad (3)$$

The boundary conditions in non-dimensional forms are

$$\begin{aligned} U = 0 \quad \theta = 0 \quad C = 0, \quad \forall y, t \leq 0 \\ t > 0; U = t^2; \theta = t; C = t; \text{ at } y = 0 \\ U \rightarrow 0, \theta \rightarrow 0, C \rightarrow 0 \text{ as } y \rightarrow \infty \end{aligned} \quad (4)$$

Let the above equations be defined as follows by non-dimensional quantities added

$$\begin{aligned} U = u' \left(\frac{u_0}{v^2} \right)^{1/3}; t = t' \left(\frac{u_0^2}{v} \right)^{1/3}; Y = y' \left(\frac{u_0}{v^2} \right)^{1/3}; \alpha = \alpha' \left(\frac{v_0}{u_0^2} \right)^{1/3}; \\ G_r = \frac{g\beta_T(T'_w - T'_\infty)}{(v u_0)^{1/3}}; S_c = \frac{v}{D_s}; A = \left(\frac{u_0^2}{v} \right)^{1/3} \\ P_r = \frac{v \rho c_p}{\kappa}; D_f = \frac{DK_T}{T_m v \rho c_p} \frac{(c'_w - c'_\infty)}{(T'_w - T'_\infty)}; \\ S_r = \frac{DK_T}{c_s c_p v} \frac{(T'_w - T'_\infty)}{(c'_w - c'_\infty)}; G_c = \frac{g\beta_c(c'_w - c'_\infty)}{(v u_0)^{1/3}} \end{aligned} \quad (5)$$

Solving the above non-similar unsteady coupled nonlinear partial differential equations from (1)-(3), under boundary conditions (4), using an explicit finite difference method (EFDM).

$$\frac{U_{i,j+1} - U_{i,j}}{\Delta t} = \frac{U_{i-1,j} - 2U_{i,j} + U_{i+1,j}}{(\Delta Y)^2} + G_r \theta_{i,j} + G_c C_{i,j} \quad (6)$$

$$\frac{\theta_{i,j+1} - \theta_{i,j}}{\Delta t} = \frac{1}{Pr} \left(\frac{\theta_{i-1,j} - 2\theta_{i,j} + C_{i+1,j}}{(\Delta Y)^2} \right) + Df \left(\frac{C_{i-1,j} - 2C_{i,j} + C_{i+1,j}}{(\Delta Y)^2} \right) \quad (7)$$

$$\frac{C_{i,j+1} - C_{i,j}}{\Delta t} = \frac{1}{Sc} \left(\frac{C_{i-1,j} - 2C_{i,j} + C_{i+1,j}}{(\Delta Y)^2} \right) + Sr \left(\frac{\theta_{i-1,j} - 2\theta_{i,j} + \theta_{i+1,j}}{(\Delta Y)^2} \right) \quad (8)$$

The original and boundary terms are then taken as follows

$$U_{i,0}^0 = 0 \quad \theta_{i,0}^0 = 0 \quad C_{i,0}^0 = \forall i, t \leq 0$$

$$t > 0; U_{0,j}^0 = (j \cdot \Delta t)^2; \theta_{0,j}^0 = j \cdot \Delta t; C = j \cdot \Delta t \quad (9)$$

$$U_{L,j}^n \rightarrow 0, \theta_{L,j}^n \rightarrow 0, C_{L,j}^n \rightarrow 0$$

Skin friction	Rate of Heat Transfer	Rate of Mass Transfer
----------------------	------------------------------	------------------------------

The velocity gradient near the plate is	The temperature gradient near the plate is	The concentration gradient near the plate is
-----------------------------------------	--------------------------------------------	----------------------------------------------

$\tau = \left(\frac{\partial u}{\partial y} \right)_{y=0}$ where	$Nu = \left(\frac{\partial \theta}{\partial y} \right)_{y=0}$	$sh = \left(\frac{\partial C}{\partial y} \right)_{y=0}$
$\tau = \frac{\tau^1}{\rho u_0^2}$		

Discussions:

For the problem, the statistical calculation of the nature of flow is taking for dissimilar actual boundaries like Dufour number, of Thermal Grash of, number of Mass Grash of, number of Schmidt, number of Prandtl, number of Soret and Time. The standard value of the number of Dufour D_f is 0.5,

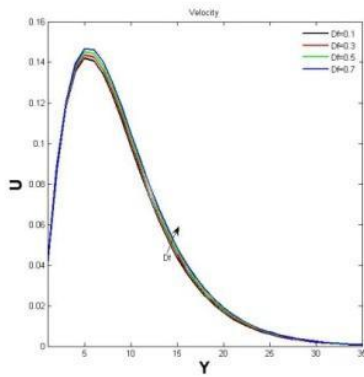


Figure 2. Acceleration shapes for several standards of D_f .

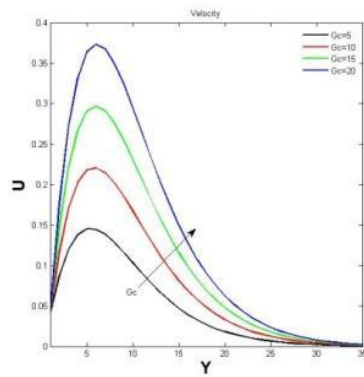


Figure 3. Acceleration shapes for several standards of G_c

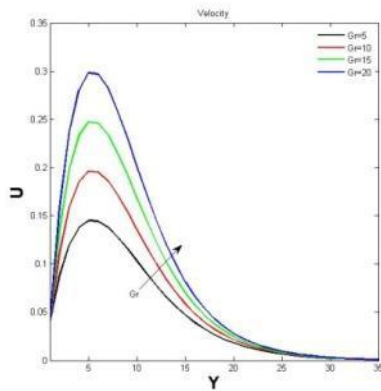


Figure 4. Acceleration shapes for several standards of G_r .

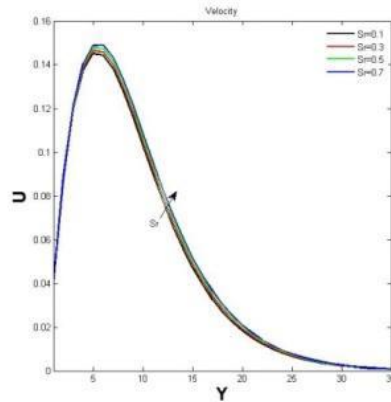


Figure 5. Acceleration shapes for several standards of S_r .

number of Thermal Grash of G_r is 5, number of Mass Grash of G_c is 5, number of Schmidt Sc is 0.22, number of Prandtl P_r is 0.71, number of Soret S_r is 0.1 and Time $-t$ is 0.2. The acceleration shapes for several standards of several parameters are presented from figure 2 to figure 8. It is detected that from figure 2 to figure 6, the acceleration shapes are rises with rising Parameters of the number of Dufour, number of Mass Grash of, number of

thermal Grash of, number of Soret and Time with respectively.

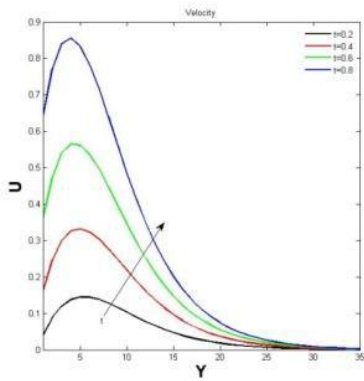


Figure 6. Acceleration shapes for several standards of t .

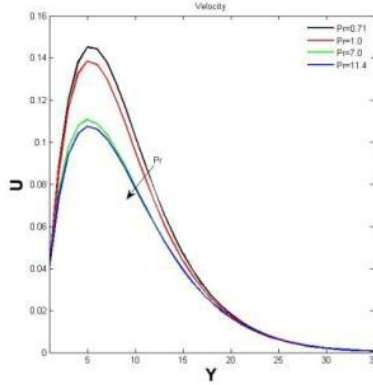


Figure 7. Acceleration shapes for several standards of P_r .

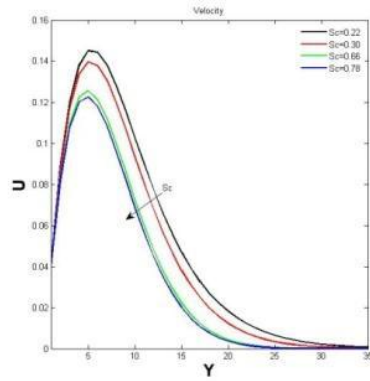


Figure 8. Acceleration shapes for several standards of S_c .

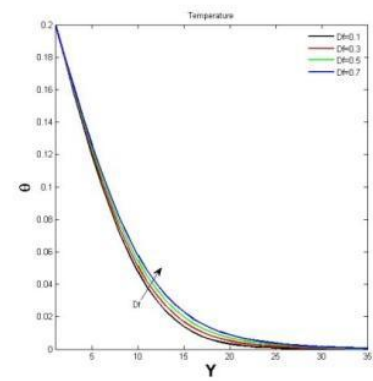


Figure 9. Temperature shapes for several standards of D_f .

Figure 7 and figure 8, it is recognized that the acceleration shapes is decreases with increasing parameters of the number of Prandtl and number of Schmidt. The Temperature profiles for different values

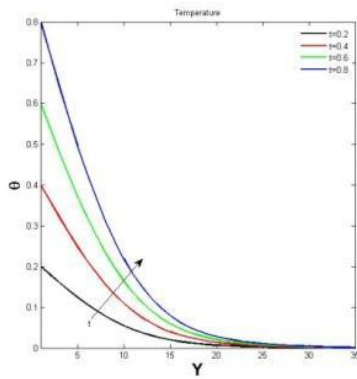


Figure 10. Temperature shapes for several standards of t .

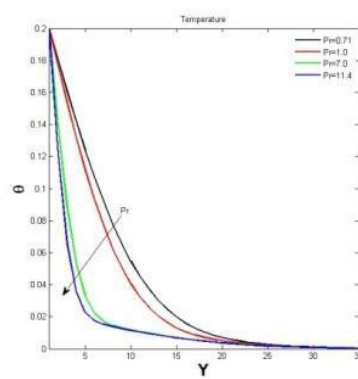


Figure 11. Temperature shapes for several standards of P_r .

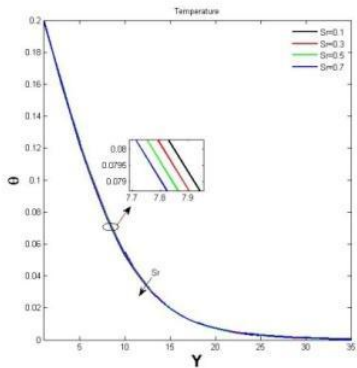


Figure 12. Temperature shapes for several standards of S_r .

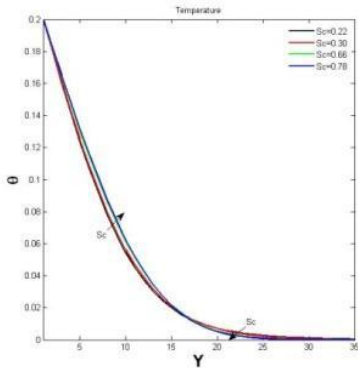


Figure 13. Temperature shapes for several standards of S_c .

of different parameters are shown from figure 9 to figure 13, It is perceived that figure 9 figure 10, the Temperature profiles are increases with increasing parameters of the number of Dufour and time. Figure 11 and figure 12 is detected that the Temperature profiles are decreases with increasing parameter number of

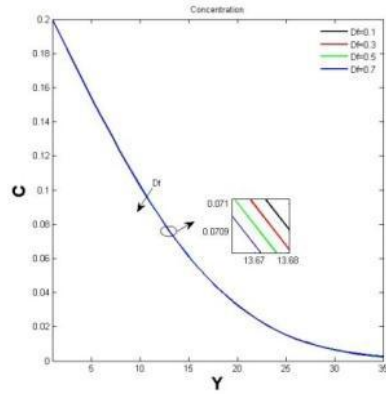


Figure 14. Concentration shapes for several standards of D_f .

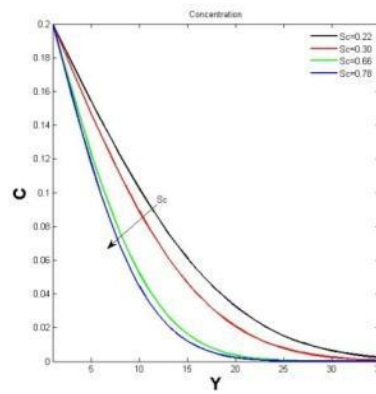


Figure 15. Concentration shapes for several standards of S_c .

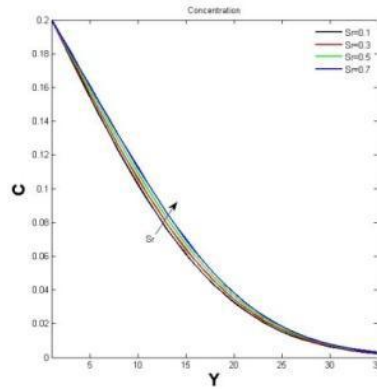


Figure 16. Concentration shapes for several standards of S_p .

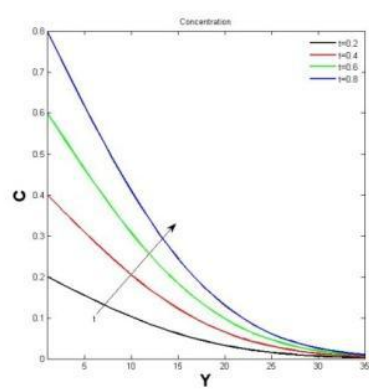


Figure 17. Concentration shapes for several standards of t .

Prandtl and number of Soret, figure 13 discerned that the Temperature profile is increases up to the crossover point after that the variation is reversed with increasing parameters of Schmidt number. Figure 14 and figure 15 illustrate that the Concentration is found to decrease with the increasing parameters number of Dufour and number of Schmidt. Figure 16 and figure 17 shows that the Concentration is

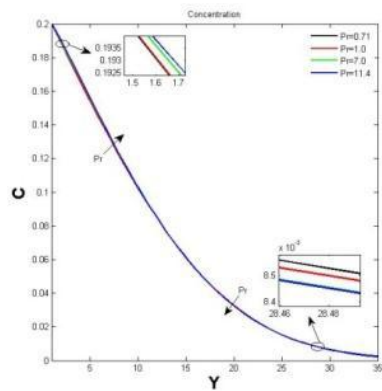


Figure 18. Concentration shapes for several standards of P_f .

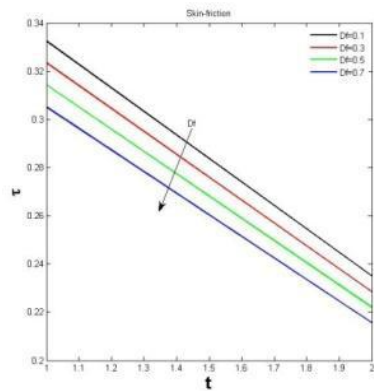


Figure 19. Skin-Friction shapes for several standards of D_f .

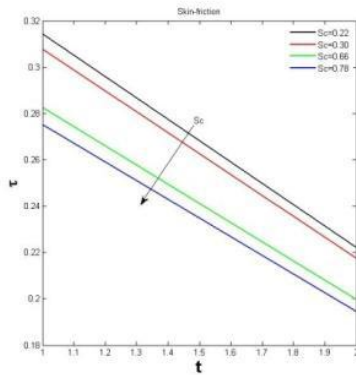


Figure 20. Skin-Friction shapes for several standards of S_c .

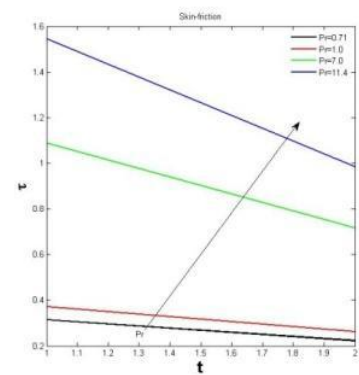


Figure 21. Skin-Friction shapes for several standards of P_f .

establish to increase with the increasing parameters number of solet and time. Figure 18 illuminate that the Temperature profile is increases up to the border point after that the variation is reversed with increasing parameters of number of Prandtl. Figure 19 and figure 20 explained that the skin-friction is decreases with increasing parameters of number of Dufour and number of Schmidt. Figure 21 and figure 22 proved that

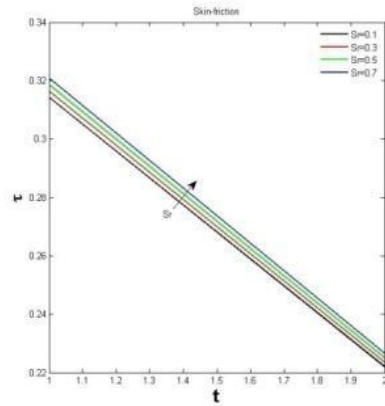


Figure 22. Skin-Friction shapes for several standards of S_r .

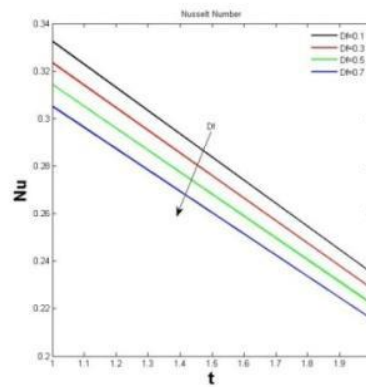


Figure 23. Nusselt number shapes for several standards of D_f .

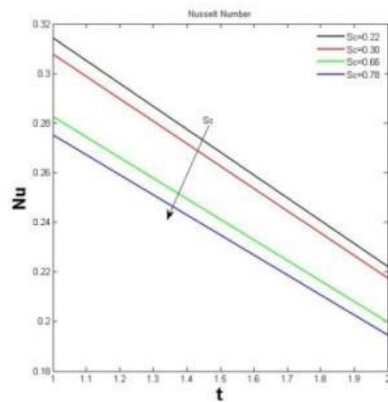


Figure 24. Nusselt number shapes for several standard of S_c .

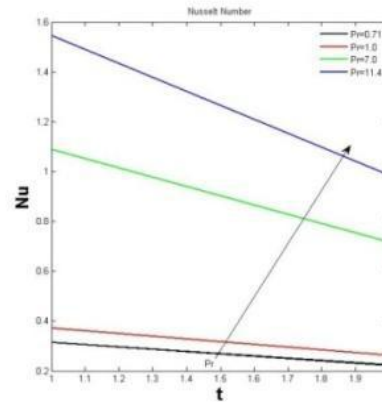


Figure 25. Nusselt number shapes for several standard of P_r .

the skin-friction is increases with increasing parameters of number of Prandtl and number of Soret. Figure 23 and figure 24 demonstrated that the skin-friction is decreases with increasing parameters of number of Dufour and number of Schmidt. Figure 25 and figure 26 exemplify that the skin-friction is increases with increasing parameters of number of Prandtl and number of Soret. Figure 27 and figure 28 demonstrated that

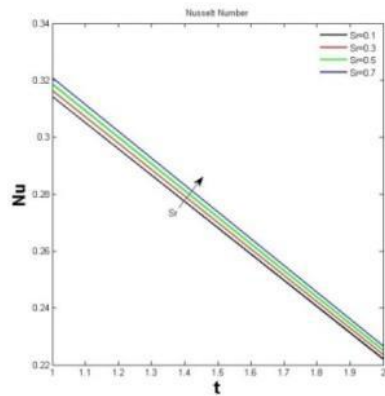


Figure 26. Nusselt number shapes for several standard of S_r .

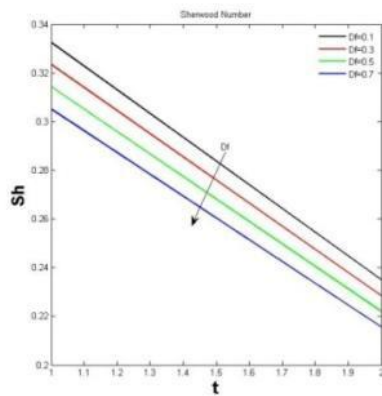


Figure 27. Sherwood number shapes for several standard of D_f .

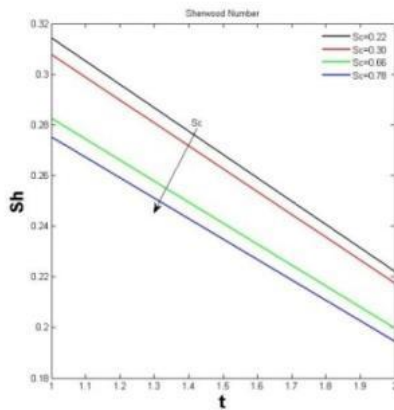


Figure 28. Sherwood number shapes for several standard of S_c .

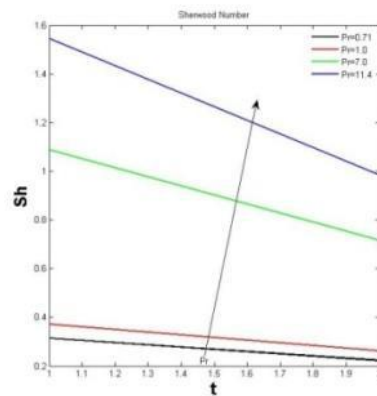


Figure 29. Sherwood number shapes for several standard of P_r .

The skin-friction is decreases with increasing parameters of number of Dufour and number of Schmidt. Figure 29 exemplify that the skin-friction is increases with increasing parameters of number of Prandtl and number.

References

[1] M. A. Hossain and L. K. Shayo, *Astrophysics and Space Science* 125 (1986), 315-324.

- [2] R. Muthucumaraswamy and A. Neel Armstrong, International Journal of Mathematical Archive-5(2) (2014), 53-58.
- [3] R. Muthucumaraswamy and P. Sivakumar, Int. J. of Applied Mechanics and Engineering 21(1) (2016), 95-105.
- [4] R. Muthucumaraswamy and M. Radhakrishnan, Journal of Mechanical Engineering and Sciences (JMES), ISSN (Print): 2289-4659; e-ISSN: 2231-8380; 3 (2012), 251-260.
- [5] R. Muthucumaraswamy, N. Dhanasekar and G. Easwara Prasad, Journal of Mechanical Engineering and Sciences (JMES) ISSN (Print): 2289-4659;e-ISSN:2231-8380; 3 (2012), 346-355.
- [6] R. Muthucumaraswamy, N. Dhanasekar and G. Easwara Prasad, Int. J. of Applied Mechanics and Engineering 18(4) (2013), 1087-1097.
- [7] R. Muthucumaraswamy and S. Velmurugan, Journal of Mechanical Engineering and Sciences (JMES),ISSN (Print): 2289-4659; e-ISSN: 2231-8380; 4 (2013), 431-439.
- [8] R. Muthucumaraswamy and E. Geetha, Ain Shams Engineering Journal 5 (2014), 1317-1323.
- [9] B. Prabhakar Reddy, Int. J. of Applied Mechanics and Engineering 24(2) (2019), 343-358.
- [10] A. K. Singh and J. Singh, Astrophysics and Space Science 97 (1983), 57-61.
- [11] V. M. Soundalgekar, Lerrers in Heat and Mass Transfer 9 (1982), 65-72.